Synergistic in vitro Antiviral Effect of Combinations of Ivermectin, Essential Oils and 18-(Phthalimid-2-yl)ferruginol Against Arboviruses and Herpesvirus

Liliana Betancur-Galvis *, Orlando José Jimenez-Jarava, Fatima Rivas, William E Mendoza-Hernández, Miguel A González-Cardenete *

Posted Date: 12 October 2023

doi: 10.20944/preprints202310.0781.v1

Keywords: Ivermectin; ribavirin; acyclovir; ferruginol; direct-acting antivirals; host-targeting antivirals; drug combinations; CHIKV; ZIKV; HHV-2.

Article

Synergistic in vitro Antiviral Effect of Combinations of Ivermectin, Essential Oils and 18-(Phthalimid-2-yl)ferruginol against Arboviruses and Herpesvirus

Liliana Betancur-Galvis [1,*], Orlando José Jimenez-Jarava [1], Fatima Rivas [2], William E. Mendoza-Hernández [3] and Miguel A. González-Cardenete [3,*]

[1] Grupo GRID- Grupo de Investigaciones Dermatológicas, Instituto de Investigaciones Médicas, Facultad de Medicina, Universidad de Antioquia, 050010 Medellín, Colombia
[2] Department of Chemistry, Louisiana State University, 133 Chopping Hall, Baton Rouge, LA 70803, USA
[3] Instituto de Tecnología Química, Universitat Politècnica de València-Consejo Superior de Investigaciones Científicas, Avda. de los Naranjos s/n, 46022 Valencia, Spain
* Correspondence: liliana.betancur@udea.edu.co (L.B.-G.); migoncar@itq.upv.es (M.A.G.-C.)

Abstract: Combining antiviral drugs with different mechanisms of action can help prevent the development of resistance by attacking the infectious agent through multiple pathways. Additionally, by using faster and more economical screening methods, effective synergistic drug candidates can be rapidly identified, facilitating faster paths to clinical testing. In this work, a rapid method was standardized to identify possible synergisms from drug combinations. We analyzed the possible reduction of antiviral effective concentration of drugs already approved by the FDA, such as ivermectin (IVM), ribavirin (RIBA) and acyclovir (ACV) against Zika virus (ZIKV), Chikungunya virus (CHIKV) and herpes virus type 2 (HHV-2). Essential oils (EOs) were also included in the study since they have been reported for more than a couple of decades to have broad-spectrum antiviral activity. We also continued studying the antiviral properties of one of our patented molecule with broad-spectrum antiviral activity, the ferruginol analogue 18-(phthalimid-2-yl)ferruginol (phthFGL). In general, the combination of IVM, phthFGL and Oregano EO showed the greatest synergism potential against CHIKV, ZIKV and HHV-2, obtaining a reduction in the EC_{99} value of up to ~8, and ~27, and ~12-fold for CHIKV, in example, respectively. The ternary combination RIBA, phthFGL, Oregano EO was slightly more efficient than the binary combination RIBA/phthFGL but much less efficient than IVM, phthFGL, Oregano EO which indicates that IVM could contribute more to the differentiations of cell targets (for example by inhibition of host heterodimeric importin IMP $\alpha/\beta 1$ complex) than ribavirin. PhthFGL showed a good pharmacokinetic profile.

Keywords: Ivermectin; ribavirin; acyclovir; ferruginol; direct-acting antivirals; host-targeting antivirals; drug combinations; CHIKV; ZIKV; HHV-2

1. Introduction

Ivermectin (IVM) is a semisynthetic mixture of two avermectin B derivatives consisting of a large macrocyclic lactone ring originally produced by the soil actinomycete, *Streptomyces avermectinius* [1]. IVM is a broad-spectrum anti-parasitic drug approved by the FDA that has also demonstrated in vitro antiviral activity against a number of DNA and RNA viruses, including severe acute respiratory syndrome coronavirus 2 (SARS-CoV-2) [2]. A systematic review published in *The Journal of Antibiotics* summarized the antiviral effects of IVM by reviewing available in vivo and in vitro studies over the past 50 years [3]. IVM exhibits antiviral activity in a variety of virus genera such as *Alphavirus, Alphainfluenzavirus, Arterivirus, Betacoronavirus, Circovirus, Flavivirus, Lentivirus, Polyomavirus, Varicellovirus*, and its main action mechanism is inhibition of host heterodimeric importin (IMP) $\alpha/\beta 1$ complex, responsible of nuclear accumulation of some viral proteins [3-6].

Essential oils (EOs) are volatile substances composed of complex mixtures of organic compounds that exhibit a wide range of biological activities, including antifungal, antibacterial, anti-larvicidal, antitumor, and antiviral properties [7]. Of particular interest are some EOs which exhibit

Preprints (www.preprints.org) | NOT PEER-REVIEWED | Posted: 12 October 2023 doi:10.20944/preprints202310.0781.v1

antiviral activity against acyclovir-resistant strains of human herpesvirus (HHV), with activity up to 100 times greater than that of acyclovir [8]. While there are numerous publications on the anti-herpetic activity of EOs and their isolated active compounds [9,10], EOs also have potential as broad-spectrum antivirals against both DNA and RNA enveloped viruses [11]. Their mechanism of action primarily involves altering the viral envelope through interactions with viral structural proteins, disrupting early stages of viral replication such as cell entry and adsorption [12,13]. Recent studies have also documented that EOs can target cellular processes, leading to differential expression of interferon response-related genes [14,15].

During our compound screening program to search new antivirals derived from natural products, it was discovered a broad-spectrum antiviral analogue of the bioactive abietane-type diterpene ferruginol (1, Fig 1.) [16,17], which we named later 12-hydroxy-N,N-phthaloyldehydroabietylamine or 18-(phthalimid-2-yl)ferruginol (**1a**, abbreviated henceforth phthFGL, Fig. 1) based on the abietane carbon skeleton numbering (Fig 1) [18-21]. PhthFGL (1a) has exhibited relevant in vitro antiviral activity against herpes and dengue [18], Brazilian zika strains [19], Colombian zika and chikungunya strains [20], and very recently, against the human coronavirus 229E (HCoV-229E) [21]. With the aim of getting insight on the possible mechanism of action of phthFGL, we carried out a basic computational study using a molecular docking approach [20]. In that work, it was found that phthFGL has a good affinity for key viral targets, including chikungunya nonstructural protein 2 (nsP2), zika and dengue virus NS5 methyltransferase; and herpesvirus thymidine kinase (TK) with a higher binding energy value than that of acyclovir itself [20]. Additionally, likewise IVM, phthFGL showed potential inhibition features towards cellular therapeutic targets, as demonstrated by its high free energy value with G-Actin and tubulin [20,22]. However, experimental evidence to confirm those predictions need to be undertaken, though some are being developed by collaborators pointing out to this molecule as a host-targeted antiviral [22]. PhthFGL is structurally an analogue of ferruginol (**1**), a well-known bioactive molecule, which possesses a phthalimide moiety attached at C18-position. Semi-synthetic bioactive abietane-type compounds are readily obtained from renewable commercial starting materials such as (–)-abietic acid, transformable into (+)-dehydroabietic acid, and (+)-dehydroabietylamine [23,24]. This makes this family of compounds very attractive for further drug development due to their broad pharmacological and drug-likeness properties and the precedent that there is only, to the best of our knowledge, one an abietane-based commercial drug, ecabet sodium (**2**, Fig. 1), available in Japan to treat acid peptic disorders [25].

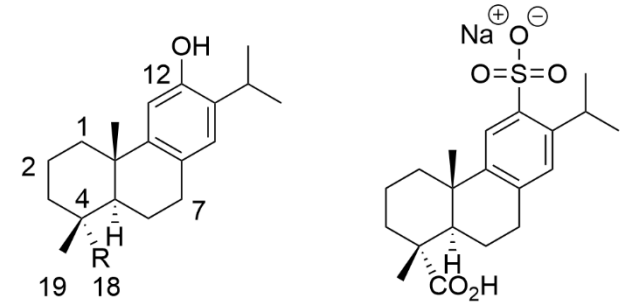

1, R = CH_3, (+)-ferruginol
1a, R = CH_2NPhth

2, ecabet sodium

Figure 1. Chemical structure of bioactive abietanes.

The combination of drugs has been historically successful for severe and chronical viral diseases such as those originated by human immunodeficiency virus (HIV), hepatitis C virus (HCV) infections and is a developing strategy for emerging or re-emerging viral diseases, including severe acute respiratory syndrome-coronavirus (SARS-CoV), Middle East respiratory syndrome (MERS)-CoV, Zika, Ebola, influenza [26]. The studies of drug-drug interactions through in vitro drug combination assays is important for several reasons. High doses of certain drugs can cause adverse effects,

 doi:10.20944/preprints202310.0781.v1

whereas combining drugs may facilitate the use of lower doses maintaining the desired therapeutic outcome or even enhanced due to synergistic effects. Additionally, combining drugs with different mechanisms of action can help prevent the development of resistance by attacking the infectious agent through multiple pathways [26]. Concurrent agents that target virus entry and virus replication, called directly acting antivirals, and cellular proteins involved in and necessary for viral replication, called host-targeting antivirals, offer opportunities to discover synergistic drug combinations [22, 27].

CHIKV and ZIKV are RNA genome re-emerging viruses who are part of the group of arboviruses, which are transmitted by arthropod vectors. These viruses have created a new challenge for public health in the Americas, with CHIKV emerging in late 2013 and ZIKV in 2014; and their infections have spread globally, causing a spectrum of disease that ranges from self-limited febrile illness to permanent severe disability, congenital anomalies, and early death [28]. Diseases caused by arboviruses such as CHIKV, ZIKV, and dengue virus (DENV) can produce very similar clinical symptoms, mainly during the acute phase (the first days of the disease), hindering clinical diagnosis by health workers, creating problems for appropriate and early case management, and sometimes triggering fatal events [28]. According to the World Health Organization, almost 4 billion people live in areas where arboviruses are current public health threats. The HHV stands out for being the main responsible for many infections in the orofacial region, as well as in the genital region. The HHV is the prototype of a large family of double-stranded DNA genome viruses; human herpesvirus (HHV) types 1 and 2 establish latent infections in sensory neurons and undergo reactivation during periods of severe host immunosuppression. Prolonged therapy with acyclovir (ACV) and its analogues can lead to drug- resistant HHV strains in patients infected with human immunodeficiency virus (HIV) [29]. Continued research in virology and pharmacology will predictably lead to the identification of new molecular targets for clinical intervention, with the objective of developing new combined treatments that will produce therapeutic synergies in the future [29,30].

Given the known antiviral properties of IVM, some EOs and phthFGL in certain viruses, we envisioned exploring the resultant antiviral activity of different combinations of IVM, Oregano or Fennel essential oils, and phthFGL. The aim of this study was the evaluation of a possible synergistic effect among them for the in vitro inhibition of the replication of Chikungunya virus (CHIKV), Herpesvirus (HHV), and Zika virus (ZIKV), as well as adverse effects reduction in our cellular model (Vero-E6 cells) determining cytotoxicity in vitro.

2. Materials and Methods

2.1. Biological Assays

2.1.1. Reagents and compounds

Dulbecco's Modified Eagle's Medium (DMEM), L-glutamine, non-essential amino acids and minimum essential medium vitamin solution, $NaHCO_3$, carboxymethylcellulose sodium salt medium viscosity (CMC) and 3-(4,5- dimethylthiazol-2-yl)-2,5-diphenyl tetrazolium bromide (MTT) were obtained from Sigma-Aldrich Chemical Co. (St. Louis, MO, USA). Fetal bovine serum (FBS) and penicillin/streptomycin were purchased from Invitrogen Life Technologies (Carlsbad, CA, USA). Ribavirin and acyclovir were obtained from Calbiochem (La Jolla, CA, USA). 18-(Phthalimide-2-yl)ferruginol (**1a**, phthFGL) was re-synthesized following details for its practical synthesis conveniently described by us [20]. PhthFGL, acyclovir and ribavirin stock solutions were prepared in dimethyl sulfoxide (DMSO, Sigma, Cream Ridge, NJ, USA) to be evaluated immediately. The essential oils (EOs) extracted from commercial aromatic plants were donated by Carmen Orozco, a distributor in Colombia of the company *doTERRA*- Essential Oils (Pleasant Grove, UT, USA). The GC-MS chromatographic analysis information was provided and the following EOs were requested: *Origanum vulgare* (Oregano) and *Foeniculum vulgare* (Fennel). The EOs have the following ID quality codes: Oregano ID 171778 and Fennel ID 161894, allowing the search of their composition on the company's website (www.sourcetoyou.com). Ivermectin 0.6% MK® (MK Drug Vademecum- 6

 doi:10.20944/preprints202310.0781.v1

mg/mL in oral solution containing excipients q.s.) was obtained from laboratory FARMATODO (Bogotá, Colombia). Both EOs and IVM were prepared in DMEM to be evaluated immediately. Before use, all reagents were kept refrigerated at temperatures no higher than 2 °C.

2.1.2. Cell culture and viruses

Vero-E6 cells (African green monkey kidney-Cercopithecus aethiops, ATCC CRL- 1586), was maintained in DMEM supplemented with 5% of inactivated fetal bovine serum (FBS), 100 units/mL of penicillin, 100 mg/mL of streptomycin, 100 mg/mL of L-glutamine, 0.14% $NaHCO_3$, and 1% of each non-essential amino acids and minimum essential medium vitamin solution (choline chloride, D-calcium pantothenate, folic acid, nicotinamide, pyridoxal hydrochloride, riboflavin, thiamine hydrochloride and i-inositol). The cells were incubated at 37 °C in humidified 5% CO_2 atmosphere for its maintenance. Zika virus_459148 (clinical isolate, Zika_virus_459148_Meta_Colombia_2016/GenBank- MH544701.2) and CHIKV were donated by the Virology Group "Dirección de Redes en Salud Pública" (Instituto Nacional de Salud, Bogotá, DC, Colombia). Zika virus_459148 characterization was described by Laiton-Donato et al., 2019 [31]. Human Alphaherpesvirus type 2, HHV-2 (VR-734), was purchased from the Center for Disease Control (Atlanta, GA, USA). Virus stocks were produced and titrated in Vero-E6 cells by plaque assay and expressed as plaque forming units (PFU/mL); or $TCDI_{50}$/0.1mL, which means the dilution of the virus required to obtained 50% lytic effect of the cellular culture in 100 µL of viral suspension. $TCDI_{50}$/0.1mL titrations were evaluated at 48 h post- infections in 96-well flat-bottomed plates and the viral stops were frozen in liquid nitrogen at concentrations of 1x 10^4 $TCDI_{50}$/0.1mL in culture medium without serum (FBS).

2.1.3. End-point titration technique (EPTT) for evaluation of IC_{99}

The technique EPTT (Vlietinck et al., 1995) [32], with few modifications was used. The unit used in the EPTT assay for three viruses (CHIKV, ZIKV, HHV-2) was of $10TCDI_{50}$, which means the dilution of the virus required to obtain 100% lytic effect of the cellular culture in well in 100 µL of viral suspension in 48 h of infection. For the evaluation of antiviral activity, initially, confluent monolayer Vero-E6 cells were grown in 96-well flat-bottomed plates (2.0 x 10^3 cells/well), at 37 °C in humidified 5% CO_2 atmosphere. After 24 h of incubation (obtaining more or less 80% of cell monolayer formed), the culture medium was removed. Then, viral suspension ($10TCDI_{50}$/0.1mL) and immediately two-fold dilutions of the compounds were added in maintenance medium, identical to growth medium except the FBS (at 1.0%). After 48 h of incubation at 37 °C in humidified 5% CO_2 atmosphere, the cell monolayers were stained with a solution of 3.5% formaldehyde with 0.2% crystal violet and cytopathic effect (CPE) was observed under inverted microscope. The minimum inhibitory concentration that does not allow to visually detect plaque formation as a cytopathic effect caused by the virus, was called the 99% inhibitory concentration (IC_{99}). Two independent experiments by triplicated for each viral type and each concentration were carried out. Controls were included: untreated cells, cells treated with compounds and cells infected with each viral type. The concentration of DMSO in assays was of 0.05% and cellular controls with DMSO at 0.05% were used. Positive controls included were: Acyclovir (ACV), Ribavirin (RIBA) and Heparin (H). The values were expressed as the Mean Standard Deviation (MSD).

2.2. In silico simulations

2.2.1. Calculation of Molecular Properties (Drug-Likeness)

The structures of compound **1a** and ecabet sodium **2** was manually drawn in ChemDraw Professional 22.2.0 software (PerkinElmer Informatics, Inc., Waltham, MA, USA), and the SMILES notation was obtained for each molecule. Then, the SMILES codes were introduced in the webserver SWISSADME [33] from the Swiss Institute of Bioinformatics (www.swissadme.ch) and calculation of physicochemical descriptors and druglike nature was performed.

 doi:10.20944/preprints202310.0781.v1

3. Results

3.1. Antiviral evaluation of IVM, EOs, phthFGL 1a against ZIKV, CHIKV and HHV-2

To evaluate the potential antiviral synergism in vitro that may arise from drug combination, it is necessary initially to determine the effective concentration that inhibits 100% of the infection in cell cultures. Additionally, to calculate a selectivity index (SI), it must be correlated with the cytotoxic concentration, i.e., the one that causes a 100% loss of cell viability. To determine the cytotoxic concentration, the crystal violet technique was used. Briefly, 2.0 x 10^3 cells/well of Vero-E6 cells were grown in 96-well flat-bottomed at 37 °C in humidified 5% CO_2 atmosphere. After 24 h of incubation, two-fold dilutions of the compounds and the respective positive controls for each evaluated virus were added. The most pertinent concentration units were used for both positive controls and molecules under study, depending on their starting state. After 48 h of incubation, the cell monolayers were stained, and the concentration that completely detached the cell monolayer, defined as the concentration cytotoxic 100 (CC_{100}), was visually identified (Table 1).

Table 1. Antiviral and cytotoxic activity of the compounds for the drug combination study.

		ZIKV		CHIKV		HHV-2	
Compounds	CC_{100}	IC_{99}	SI	IC_{99}	SI	IC_{99}	SI
1a, µM	410	25,6	16	25,6	16	25,6	16
IVM, µg/mL	6.4	1,2 ± 0,4	5,3	1,8 ± 0,6	3,5	3,2*	2
Oregano, ppm	18,6 ± 0,6	8	2,3	3,6 ± 0,7	5,1	5,3 ± 1,8	3,5
Fennel, ppm	64	12 ± 4	5,3	14,6 ± 2,9	4,4	12 ± 4	5,3
RIBA, µM	>700	176	>4	44	>16	176	>4
ACV, µM	>660	NT	--	NT	--	6,6	>100
Heparin, U.I/mL	640	NT	--	NT	--	10	64
RIBA/ACV 1.3 µM	NT	NT	--	NT	--	36,6 ± 10	--

CC_{100}: 100% cytotoxic concentration; SI: selectivity index; NT: no tested; -- : No calculated; * : IVM was able to inhibit the cytopathic effect to approximately 50%, but at a concentration that showed a reduced cell monolayer.

The same protocol was used to evaluate the antiviral concentration that inhibits 100% of the cytopathic effect; with an additional step, of infecting the cell monolayer with 10$TCDI_{50}$ of the respective virus before adding non-cytotoxic two-fold dilutions of the compounds (these two steps were performed almost simultaneously). The minimum inhibitory concentration that did not allow visualizing plaque formation as a cytopathic effect caused by the virus, was called the 99% inhibitory concentration (IC_{99}) (Table 1). Using IC_{99} has many advantages over the IC_{50}; IC_{99} reduces the number of experiments, eliminates the need to ensure a dose-dependent effect, and is a fast and inexpensive method that does not require additional statistical analysis. Previously, the antiviral activity of each compound must be known, ensuring 100% inhibition of the cytopathic effect through visual determination (and dose- dependent effect). The methodology standardized here is only an approximation, equivalent to a "synergism screening" where synergism controls should be included in the experimental design. As a positive synergism control, we included the combination of RIBA with ACV in the viral model of HHV-2, a synergism that has been documented by several studies [34,35]. As can be seen in Table 1, the IC_{99} of RIBA, in the presence of ACV (at the concentration of 1.3 µM), was reduced from 176 to 36.6 µM, a reduction that is equivalent to more than four times its initial concentration. This parameter of "more than four times" was chosen as threshold when analyzing the possible synergism in the binary or ternary combinations tested in this study. As shown in Table 1, the tested compounds IVM, **1a** and EOs have lower SI values than the selected positive controls ACV and Heparin. IVM had the lowest selectivity index (of 2 against HHV-2), while phthFGL (**1a**) showed the highest IC_{99} value (SI = 16). Broad-spectrum antiviral activity has already been demonstrated for EOs, but in this particular case, by Oregano and Fennel EOs is the first time that their antiviral activity is reported for both HHV-2 and arboviruses. It is the same way, it the first time that IVM showed activity against HHV-2 replication; but IC_{99} value could not be determined,

Preprints (www.preprints.org) | NOT PEER-REVIEWED | Posted: 12 October 2023 doi:10.20944/preprints202310.0781.v1

since it was close to the CC_{100} value. In following experiments, binaries combination or three compounds were realized to demonstrate whether the 100% inhibitory effect is maintained with a reduction of concentration. The increase of SI also was analyzed.

3.2. Antiviral evaluation of binary and ternary combinations of compounds

In Figure 2, the experimental design with the HHV-2 viral model is shown. Briefly, viral titer control is found in the lower left panel, which consisted of two-fold dilutions, starting at 1TCDI50 and finalizing in the 1/16 TCDI50 dilution, with an average of 3.7 plaque-forming units per well. Lower right panel was the cell control. The upper left panel shows the cytopathic effect of the double serial combination of three compounds, corresponding to the mixture of IVM, Oregano EO and phthFGL (**1a**). The IC_{99} data recorded per three replicates, for each compound, in this quadrant were: Oregano EO, 0.2, 0.2, 0.5 ppm; IVM, 0.2, 0.2, 0.4 μg/mL and phthFGL (**1a**), 0.8, 0.8, 1.6 μM. The replicates for next quadrant corresponding to binary combinations IVM and phthFGL (**1a**), were: IVM, 0.8, 0.8, 0.8 μg/mL and phthFGL (**1a**), 3.2, 3.2, 3.2 μM. The IC_{99} of binary combinations of IVM and Oregano EO were: IVM, 0.8, 1.6, 1.6 μg/mL and Oregano EO 0.5, 1.0, 2.0 ppm (quadrant that is found below the quadrant of the binary combination of IVM and phthFGL (**1a**). The other quadrants correspond to the treatments with a single compound (the IC_{99} average concentrations are already reported in Table 1). Three-component combinations reduced IC_{99} concentration more than binary combinations. Two experiments by triplicate for each viral type and each concentration (binary and three-component combinations) were tabulated and graphed with their standard deviation as shown in Figures 3, 4, 5.

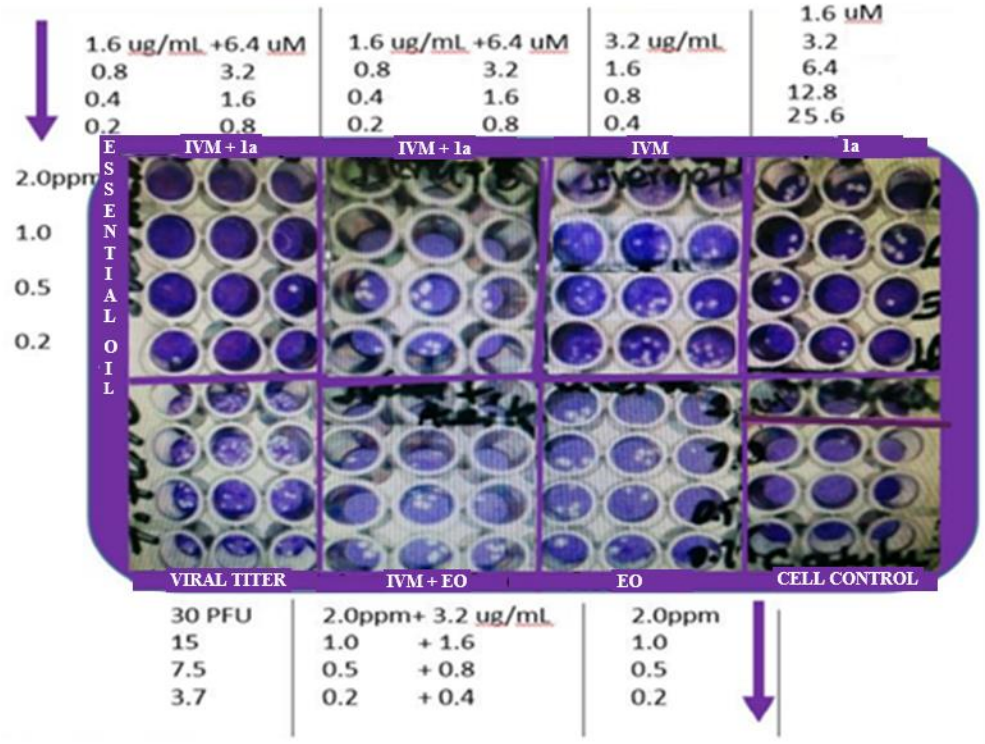

Figure 2. Experimental design for synergism determination.

3.2.1. Antiviral activity of IVM or phthFGL (1a) in the context of combinations against HHV-2, CHIKV and ZIKV.

In Figure 3A (see below), the IVM concentration in μg/mL is plotted on the Y-axis, and the order of presentation on the X-axis is as follows: IVM, IVM/**1a**, IVM/Oregano, IVM/Fennel, IVM/(**1a** + Oregano) and IVM/(**1a** + Fennel). The figure 2A shows that binary combinations reduced the IVM inhibitory concentration, being combination IVM/Fennel the one with least effect. In the last two bars, the IVM/(**1a** + Fennel) combination gave approximately the same effect than binary combination

Preprints (www.preprints.org) | NOT PEER-REVIEWED | Posted: 12 October 2023 doi:10.20944/preprints202310.0781.v1

IVM/**1a**. The effect of the combination of IVM/(**1a** + Oregano) was greater than any binary combinations. It should be noted that IVM alone was not able to inhibit 100% of lysis plaque formation by HHV-2 infection (the bar represents approximately the 50%); this was only possible on combining with other compounds. On comparing the binary and the ternary combinations of agents, it can be observed that the big difference in the reduction of IC_{99} is made by the contribution of Oregano EO in the combination of the three components. In figure 3B, compound **1a** concentration's in μM is plotted on the Y-axis, and the order of presentation on the X-axis is as follows: **1a**, **1a**/ IVM, **1a**/Oregano, **1a**/Fennel, **1a**/RIBA, **1a**/ACV, **1a**/(IVM + Oregano) and **1a**/(IVM + Fennel). The binary combinations of **1a** with IVM, Oregano EO, Fennel EO, RIBA and ACV reduced the IC_{99} of compound **1a** generally around five times from 25.6 to c.a. 5 µM. The three component **1a**/(IVM + Oregano) and **1a**/(IVM + RIBA) mixtures, reduced the concentration much more at values below 5 µM; the oregano-based ternary mixture including IVM makes the big difference in the reduction power of IC_{99}. For combinations of three compounds, the order of higher effect was: **1a**/(IVM+ Oregano) > **1a**/ (Oregano+ RIBA) > **1a**/(IVM+ Fennel). The IC_{99} reduction by binary and/or three-component combinations was more evident when the analysis was done from **1a** (Fig. 3B), this could be because **1a** has the highest value of IC_{99} concentration, and the two-fold dilutions used show per se a greater effect (12.8, 6.4, 3.2, 1.6, 0.8, 0.4). Control drugs (RIBA and ACV) were combined with **1a**; both compounds reduce the IC_{99} of **1a** from 25 µM to approximately 5 µM. In the following experiments for the CHIKV and Zika viral models, only RIBA was used as control since this drug possess broad-spectrum properties.

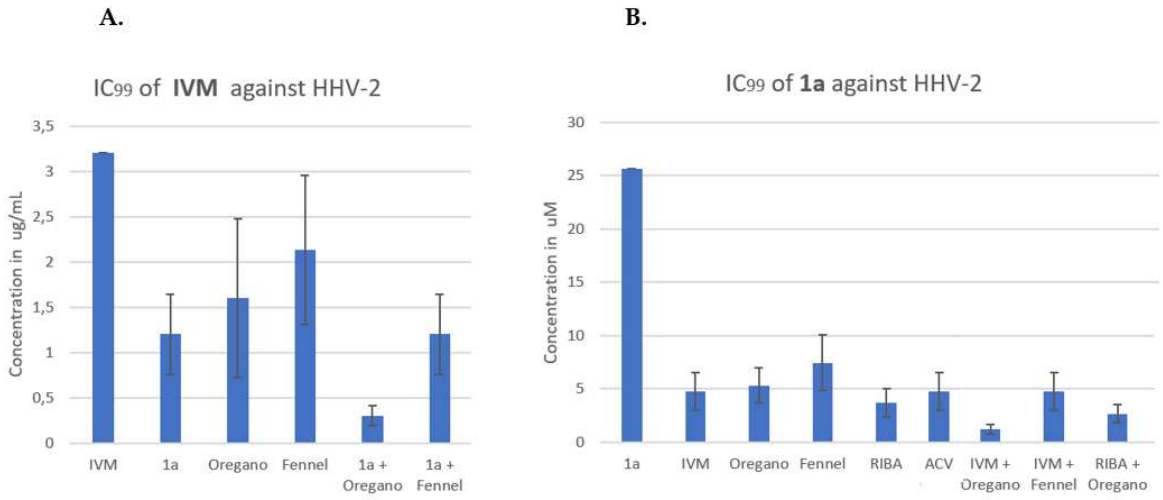

Figure 3. Reduction of IC_{99} inhibitory concentration of IVM (Fig. 3A) or compound **1a** (Fig. 3B) against HHV-2 virus in binary and ternary combinations.

CHIKV (with an RNA genome) was another viral model for the study of binary and three-component combinations (Fig. 4), which was much more sensitive to the binary combination of IVM/**1a** than HHV-2 (Figure 4A/ second column)). IVM had an IC_{99} of 1.8 µg/mL (Table 1, Figure 4A/first column), and the reduction of this concentration in the binary combination with IVM/**1a** and IVM/Oregano EO was below 1.0 µg/mL. The combination of IVM/Fennel EO was the least effective, as it was also in the case of the three-component combination of the latter with **1a**. Also, the effect of the combination of IVM/Oregano EO + **1a** was greater than that of IVM/Fennel + **1a**. As stated for Figure 3B, when making the respective analysis with **1a**, the figure 4B shows the same tendency for both the binary and three-component combinations. However, in this case, CHIKV is more sensitive to the binary combination **1a**/Oregano EO than **1a**/Fennel EO.

Preprints (www.preprints.org) | NOT PEER-REVIEWED | Posted: 12 October 2023 doi:10.20944/preprints202310.0781.v1

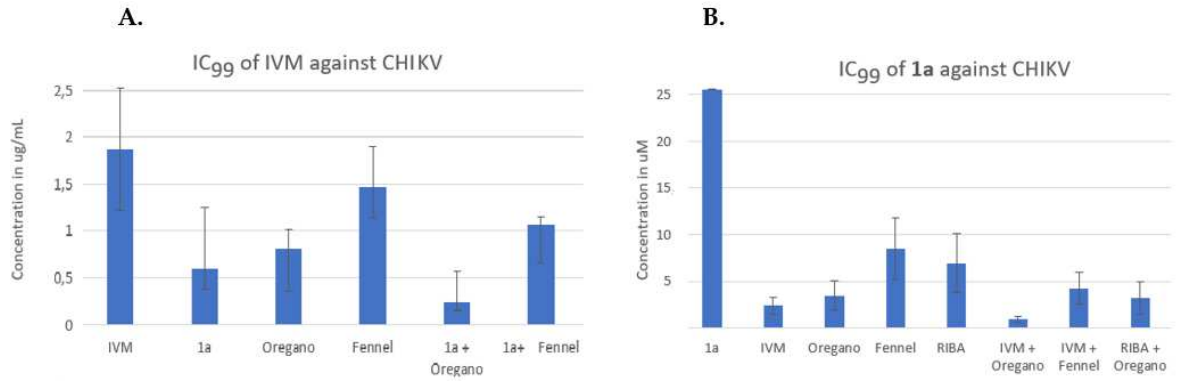

Figure 4. Reduction of IC_{99} inhibitory concentration of IVM (Fig. 4A) or compound **1a** (Fig. 4B) against CHIKV in binary and ternary combinations.

Another RNA genome model, ZIKV, was also studied resulting to be less sensitive than CHIKV, but of all the binary combinations, the one containing Oregano EO was the most effective to reduce IC_{99} of IVM (Fig 4A). Also, the effect of the combination of IVM/**1a** + Oregano EO was greater than the other ternary mixture, IVM/**1a** + Fennel. In figure 4B, the respective analysis with compound **1a**, is depicted. In this case, ZIKV was just as sensitive as CHIKV. But the effect of the combination of **1a**/ RIBA + Oregano EO was less sensitive than that of **1a**/IVM + Fennel. For the combinations of three agents, it was observed the following decreasing order of efficiency: **1a**/(IVM+ Oregano) > **1a**/(IVM+ Fennel) > **1a**/Oregano + RIBA.

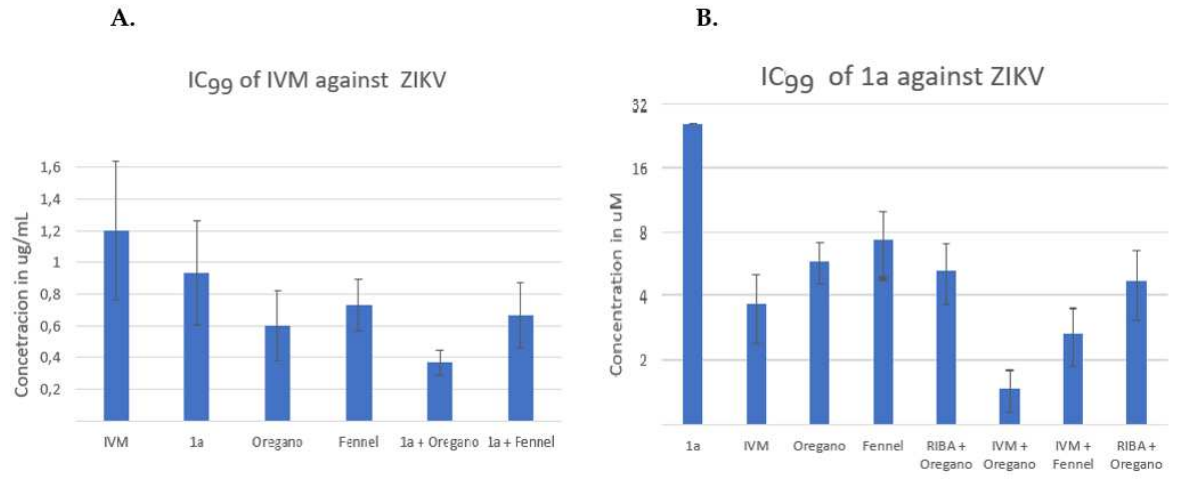

Figure 5. Reduction of IC_{99} inhibitory concentration of IVM (Fig. 5A) or compound **1a** (Fig. 5B) against ZIKV in binary and ternary combinations.

3.2.2. Reduction of IC_{99} values in comparison with ACV/Ribavirin as synergism control.

To have the same unit of comparison to evaluate the synergisms, the Y-axis was changed by the number of times that the IC_{99} value was reduced. The figure 6 shows the effects of possible synergies, comparing the three viral models. The synergism control or minimum threshold was the RIBA/ACV system, which reduced the IC_{99} value around four times in the HHV-2 model. Thus, any combination that reduces the IC_{99} value by more than four times will be considered as a mixture with a potential synergism effect. In figure 6A, the IC_{99} reduction values for antiviral activity against the HHV-2 virus, is shown. The experimental design and the way of graphing the results allowed us to discriminate which of the evaluated combinations had greater evidence of synergism. The control: ACV + RIBA and ACV + **1a**, RIBA + **1a** were near the 5-fold threshold line, except compound **1a** mixed with ACV (Fig. 6A). The binary combinations: IVM + Fennel and **1a** + Fennel were also below the 5-fold threshold line. The combination of three components that reduced the greatest number of times the

Preprints (www.preprints.org) | NOT PEER-REVIEWED | Posted: 12 October 2023 doi:10.20944/preprints202310.0781.v1

IC_{99} value against HHV-2 was: IVM + **1a** + Oregano EO, with reductions of more than ten, twenty and fifteen times, respectively. The combination RIBA+ **1a** + Oregano EO was slightly larger than the binary combination RIBA + **1a**, but much smaller than IVM + **1a** + Oregano, which indicates that the action mechanism of IVM (inhibition of host heterodimeric IMP $\alpha/\beta 1$ complex) could related to higher contribution to certain cell targets to what RIBA does.

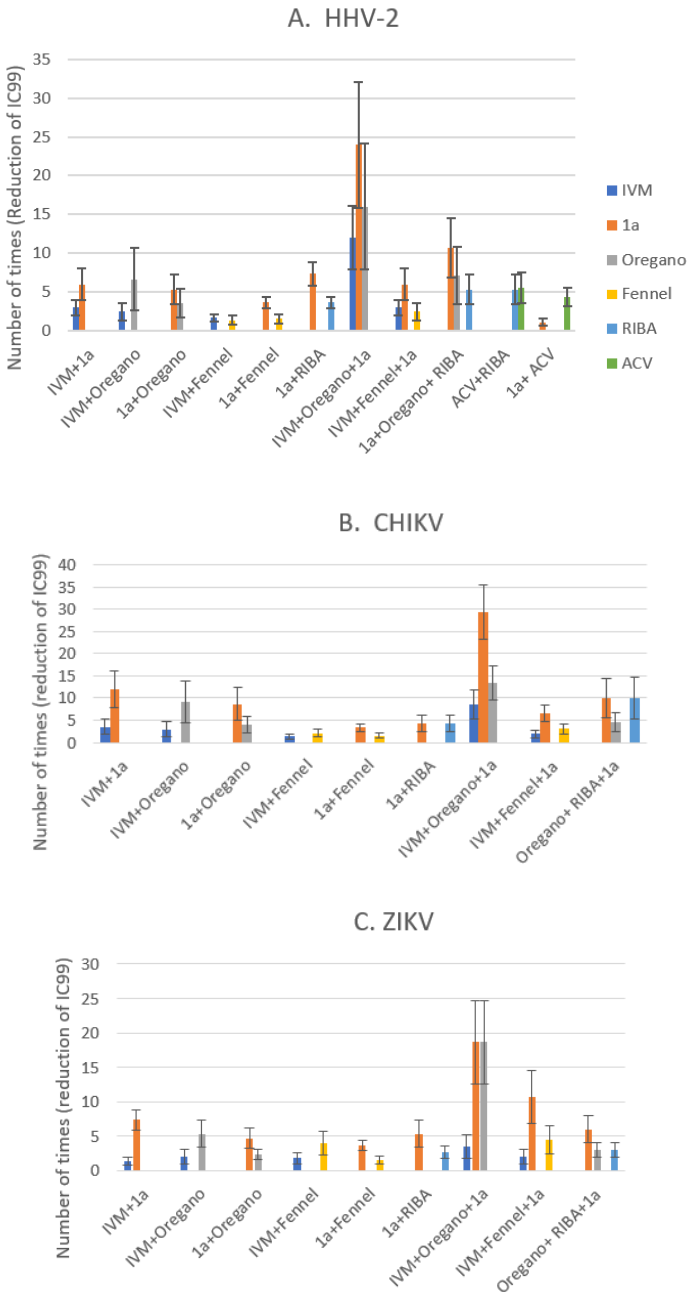

Figure 6. Reduction of IC_{99} inhibitory concentration (number of times) for the different models (Fig. 6A, HHV-2), (Fig. 6B, CHIKV) and (Fig. 6C. ZIKV in binary and ternary combinations.

The model of RNA genome, CHIKV, has been the one that showed the greatest sensitivity at synergism, as can be seen in the combination of three components, where **1a** IC_{99} value was reduced more than twenty-five times (Fig. 6B). Unfortunately, all binary combinations were below the 5-fold threshold line; except those containing compound **1a** where the synergism produces a reduction of the IC_{99} value from five to ten times, when it was mixed with Oregano EO or IVM, respectively. In the same way as it was shown with the HHV-2 model, the differences between the two EOs are conserved in the CHIKV model, with Oregano EO-containing mixtures displaying the greatest

 doi:10.20944/preprints202310.0781.v1

interaction to promote synergism. On the contrary, the ZIKV model was the least sensitive for the reduction of the IC_{99} value, falling almost all the binary combinations below of the 5-fold threshold (Fig. 6C), except with compound **1a** that reduced more than five times the IC_{99} value when was mixed with IVM. In the discussion section, the plausible mechanism of action that has been evaluated so far for compound **1a** will be analyzed, considering what is known about its cellular or viral targets with respect to targets of the other compounds tested. If we compare the two RNA genome models, there are differences in the results obtained by the combination of three components, mainly when the difference in the mixture was the EO used. Besides, for viruses of RNA genome, it can be concluded that Oregano EO–containing mixtures presents a greater reduction in IC_{99} values, which suggests that the chemical composition of Oregano EO possibly influences more synergism in the routes used by the CHIKV and ZIKV for its replication than those of HHV-2.

The composition of the EOs was analyzed and reported by the company "doTERRA" for the batch supplied (Oregano ID 171778 and Fennel ID 161894, company website www.sourcetoyou.com). Briefly, the major components of Oregano EO versus fennel EO are: 74.2% carvacrol vs. 74.5% trans-anethole. The minor components are respectively: for Oregano EO, linalool, thymol, beta-caryophyllene, terpinene-4-ol, alpha and gamma-terpinene; and for Fennel EO, limonene, alpha-pinene, fenchone, methyl-chavicol and beta-caryophyllene.

4. Discussion

Due to the high costs associated with drug development, there is a priority to search new strategies. One of them is drug combination therapies to combat emerging viral infections, among other type of diseases. By using faster and more economical screening methods, candidates with "effective synergies" could be rapidly identified, facilitating or to made faster paths to clinical testing [26,27]. IVM is a specific inhibitor of the importin-α/β-dependent nuclear transport protein complex (IMPα/β1) and has shown potential antiviral activity against several RNA and DNA viruses [2-6]. For example, IVM's antiviral action on coronavirus is explained as follows: during SARS-CoV-2 replication, the IMPα/β1 complex binds to coronavirus cargo proteins in the cytoplasm translocating them through the nuclear pore complex (NPC) to the nucleus [2,6]. There, the viral proteins reduce the antiviral response of the host cell, leading to enhanced infection [2-6]. IVM dissociates preformed IMPα/β heterodimers, which are required for the nuclear import of coronavirus proteins. This prevents IMPα/β1 from binding to viral proteins and entering inside the nucleus [6,36]. Caly et al., 2020 [2] tested IVM's antiviral activity against SARS-CoV-2 (Australia/VIC01/2020 isolate) in Vero/hSLAM cells at a multiplicity of infection (MOI) of 0.1 (48 hpi) resulting in an EC_{50} value of ca. 2.0 μM [2]. High doses of 600 μg/kg/day of IVM in humans have shown to produce a maximum plasma concentration (Cmax) of 120 ng/mL [37], which is much lower than its in vitro antiviral value of ~2 μM [2]. This could be supported with simulation studies obtained in mathematical models which have estimated that IVM achieves lung tissue concentrations up to three times higher than plasma concentrations [37]. However, a 5-day treatment with 12 mg once daily of IVM in adults showed viral clearance in SARS-CoV-2 patients at 9.7 days compared to 12.7 days in the placebo group [38]. Moreover, in a clinical study with dengue patients (DENV4 / 45.2%, DENV3 / 33.9%, DENV2 / 8.7%, and DENV1 / 7.0%), a daily oral dose of 400 μg/kg of IVM also showed a trend towards a reduction in plasma nonstructural protein 1 (NS1) clearance at day 3 compared to placebo, though clinical efficacy was not observed at that dose regimen [39]; even though in vitro, IVM EC_{50} values for DENV/1-4 ranged from 1.6-2.3 μM in BHK-21 cells (48 h p.i) [40]. To date, it remains a discrepancy regarding the applicability of IVM as a broad-spectrum antiviral treatment due to its low plasma levels achieved with oral treatments. For this reason, drug combination synergism may be a plausible alternative [41-42], as well as innovations in administration routes (such as nasal spray formulations [43]) to enhance its effectiveness.

In this study, we have standardized a rapid method to identify possible synergisms from drug combinations analyzing the possible reduction of effective antiviral concentration of IVM and other candidate molecules already approved by the FDA. EOs were included in the study because they have been reported for more than a couple of decades to have broad-spectrum antiviral activity [10-

 doi:10.20944/preprints202310.0781.v1

15]. We added in the experiments one of our patented molecules with demonstrated broad-spectrum in vitro antiviral activity [20], the abietane-derived analogue, 18-(phthalimide-2-yl)ferruginol (phthFGL) (1a, Fig. 1), as a continuation of our studies on this "wonder" molecule. In the light of the present research, evidence of broad-spectrum antiviral activity (against ZIKV, CHIKV, and HHV-2) of different combinations of three molecules (IVM, RIBA, phthFGL) and two EOs (Oregano and Fennel), is reported. IVM had already shown activity against ZIKV and CHIKV [6,44]. We found an IC_{99} value of c.a. 1.2 μg/mL (1.37 μM) for ZIKV in a period of 48 hpi (10$TCDI_{50}$/~ MOI= 1). Also, Varghese et al., (2015) [44] reported an anti-CHIKV IC_{50} value of 0.6 μM in BHK-21 cells at 16 hpi/MOI= 0.01; while the CHIKV IC_{99} value obtained by us was of 1.8 μg/mL (2.1 μM). To the best of our knowledge, IVM has not been studied against HHV-2 until now. In this study, IVM was less active against HHV-2 than against ZIKV and CHIKV. Słońska et al., (2013) [45] evaluated the antiviral activity of IVM against two strains of equine herpesvirus type 1 (Jan-E EHV-1 and Rac-H EHV-1) but only antiviral activity against the Jan-E EHV-1 strain was found. Lv et al., (2018) also investigated the role of IVM on virus replication of a subfamily alpha-Herpesviridae such as pseudorabies virus (PRV) [46]. They found that IVM at 2.5 μM disrupted the nuclear localization of PRV UL42 (accessory subunit of PRV DNA polymerase) in a BHK-21 cell line model, by targeting the nuclear localization signal of the proteins and decreased PRV titers by more than 7000-fold after 48 h of viral infection [46]. Döhner et al., 2018 suggest that importin α1 protein is specifically required for the nuclear localization of several important HHV-1 proteins involved in processes such as capsid assembly and capsid egress into cytoplasm [47]. In our study, we found that IVM had antiviral activity against HHV-2 at concentrations below 3.2 μM, reaching approximately up to 50% inhibition. It was not possible to find an EC_{99} concentration because its value was close to the cytotoxic concentration in our experimental model (commercial-IVM/Vero E6 cells). Our results of antiviral activity of IVM against HHV-2, allow to assume that a subfamily of alpha-Herpesviridae, the HHV-2, use nuclear carriers for their viral proteins as it has been shown by other researchers for related viruses [45-47].

PhthFGL (**1a**, Fig. 1) is an abietane-derived analogue of (+)-ferruginol (**1**, Fig. 1) similar structurally to the commercial drug Ecabet sodium (**2**, Fig. 1) [20,48]. To date, ecabet sodium is the only commercial drug based on abietane-type diterpenoids which it is clinically used in the treatment of gastritis and gastric ulcer in Japan, since possesses high affinity to gastric adherent mucosa, epithelial cells, albumin, and fibrinogen in the ulcer region [48]. Volunteers following a single oral administration of an ecabet disodium tablet (1 g) showed a plasma maximum concentration-time profile of 4926 ± 880 ng/mL at the first hour and a plasma elimination half-life of 6.63 ± 2.24 h [48,49]. Meanwhile, for ferruginol (**1**, Fig. 1), pharmacokinetic studies have been performed in rats obtaining a maximum concentration in plasma of 3140 ng/mL at 40 min after oral administration at a dose of 20 mg/kg (~ 1 g in adults), and a plasma elimination half-life of 41.73 min [50]. In silico modelling of drug-likeness, such as Lipinski's rules have reported that both ferruginol and phthFGL violate only one rule, which corresponds to the partition coefficient (their values are 6.41 and 7.08 respectively, and it cannot be greater than 5) [21]. In addition, in silico modelling prediction of toxicity, using Gosselin, Smith, and Hodge scale, gave that phthFGL possess a reasonably good safety profile by oral administration in rats [21]. The LD_{50} value for phthFGL expressed as the weight of the chemical per unit of body weight was in the range of $500 < LD_{50} \leq 5000$ mg/kg being moderately toxic. According to the organization for economic co-operation and development (OECD) manual was classified as class 4 [21]. During different research studies, we have reported the antiviral activity of phthFGL against DENV-2 and HHV-2 [18], ZIKV [19,20], and CHIKV [20]. This interesting molecule displayed EC_{50} values in the range 1.0-20.0 μM for those viruses, specifically, of 1.4 μM for DENV-2, and 19.2 μM for HHV-2 [18], of 7.7 μM for a Brazilian Zika strain (clinical isolate, IMT17)[19], of 5.3 μM for COL345Si Zika, 6.3 μM for Zika_459148, and 9.8 μM for CHIKV [20]. Very recently, we demonstrated that was also active against human coronavirus HCoV 229E (PHE/NCPV 0310051v) where a IC_{99} value of 3.0 μg/mL (6.9 μM) was found [21]. In the experimental design of this study, double serial dilutions were used from 0.4 to 25.6 μM for phthFGL, resulting in IC_{99} values of 25.6 μM for the three tested viruses ZIKV, CHIKV and HHV-2. Unpublished studies strongly suggest that in the antiviral mechanism of action of phthFGL are implicated the disruption of the viral

 doi:10.20944/preprints202310.0781.v1

polyproteins translation, via the alteration of actin remodeling, as well as other related cellular and viral processes involved in the replicative complex formation [18,22].

DeForni et al (2022) [51] evaluated the effect of combining of IVM, remdesivir (RDV) and azithromycin (AZI) on SARS-CoV-2 replication in vitro. In that study, a two-dimensional matrix of 49 different combinations to quantify synergistic interactions was created to validate synergistic concentrations. They mixed two-fold serial dilutions of compounds with Vero E6 cells (~70% confluence), in 96-well assay plates; 1 hour later, the cells were infected with SARS-CoV-2 at a multiplicity of infection MOI= 0.01. These researchers found that combining RDV and IVM led to lower concentrations to achieve a complete inhibition (~IC_{99}), specifically 6- and 13-fold for RDV and IVM, respectively [51]. In a similar manner, we also used two-fold serial dilutions of compounds (IVM and phthFGL or Oregano or Fennel EOs) and mixed with 10TCID50 of each virus (CHIKV, ZIKV and HHV-2). Then, these mixtures were added to 96-well assay plates when Vero E6 cells reached ~80% confluence. The IVM and phthFGL combination led to a much lower IC_{99}s than either single treatment or IVM combined with Oregano or Fennel EOs. The combined IC_{99} of IVM and phthFGL against HHV-2 was of 1.2 ± 0.4 vs >3.5 μg/mL with only IVM (Fig. 3A), while for CHIKV the IC_{99} was of 0.6 ± 0.2 μg/mL vs 1.8 ± 0.6 μg/mL (Fig. 4A), and for ZIKV the IC_{99} was of 0.93 ± 0.3 vs 1.2 ± 0.4 μg/mL (Fig. 5A), in this drug combination regimen. The synergism controls such as RIBA and ACV were used to validate the results obtained with our own experimental design [34,35]**.** RIBA and ACV were evaluated against HHV-2 as a positive control for the model of "potentiating effect" o synergism since the two drugs exhibits complementary mechanism of action [34,35]. On the one hand, it is known that ACV is selectively phosphorylated by herpes simplex virus (HHV)-encoded thymidine kinase and then, cellular enzymes catalyze the conversion of ACV-monophosphate to its triphosphate form (ACV-TP) [52]. ACV-TP inhibits viral DNA synthesis and also leads to inactivation of the HSV-l-encoded DNA polymerase [52]. On the other hand, RIBA, among other mechanisms, inhibits the synthesis of guanosine monophosphate consequently reducing the intracellular guanine nucleotide pool (GTP and dGTP, natural counterpart of ACV-TP,[52]); action that may explain the antiviral activity against both DNA and RNA viruses [34,35,52]. In the HHV-2 viral model, the IC_{99} for RIBA was reduced from 176 μM to 36.6 ± 10 μM, when it was combined with ACV, while for ACV the IC_{99} decreased from 6.6 μM to 1.3 ± 0.4 μM, which is the c.a. 5-fold threshold in the synergism determinations (Fig. 6A). Pancheva et al. (1991, 1990) found an IC_{50} reduction to 40 μM by RIBA combined with ACV (1.1 μM) against HHV-1 [34,35], those results agree with what we obtained in our experimental design for these two controls. Moreover, RIBA combined with phthFGL (**1a**) reduced its IC_{99} value from 176 μM to 51.3 ± 39 μM while for ACV the IC_{99} value decreased from 6.6 μM to 1.87 ± 0.6 μM. Therefore, the most favorable binary combination to reduce the IC_{99} value was the one presented with **1a**, even when it was evaluated together with RIBA (25.6 μM vs 3.73 ± 1.19 μM). Experimental studies carried out by us [10], and other researchers [12,13,53,54] indicate that EOs interfere with virion envelope structures masking viral envelope proteins, which are necessary for adsorption and entry into the host cell. Mediouni et al., (2020) [53] found that the anti-HIV-1 activity of Oregano EO depends both on the composition, logically, and on the virus envelope. The anti-HIV-1 activities of the main Oregano EO components, carvacrol and its isomer thymol and their mixtures, were explained as a virucidal activity, where these components inactivated the virus binding site (glycoprotein binding peptide) of viral gp120 to its host cell [53]. Carvacrol, also changes the proportion of cholesterol present in the viral envelope (or cell membranes) [53,54]. It has been shown that the virus modulates the cholesterol metabolism during viral cycle affecting the intracellular cholesterol homeostasis [53-57]. Therefore, low cholesterol levels emerge as a novel broad-spectrum antiviral strategy, though evidence accumulates that withdrawal of cholesterol hampers innate immunity [56]. Based on this background, it was decided to include EOs in our synergism studies. From a previous study of the antiviral activity of more than thirty EOs from species of the Verbenaceae, Piperaceae, Poaceae, Lamiaceae, Lauraceae and Myrtaceae families against ZIKV, DENV, CHIKV, HHV-2 and HHV-1 viruses of which only results against CHIKV have been published [58], the Oregano and Fennel EOs were selected for the present study. The *Origanum*

 doi:10.20944/preprints202310.0781.v1

vulgare (Oregano) and *Foeniculum vulgare* (Fennel) EOs from doTERRA company showed virucidal activity with broad-spectrum antiviral properties.

In this study, the combination of IVM, phthFGL and Oregano EO showed the greatest synergism potential with higher values for CHIKV than ZIKV and HHV-2, obtaining a reduction in the EC_{99} value of up to ~8 and ~27-fold for IVM and phthFGL, respectively, while for Oregano EO the reduction was of ~12-fold. The synergism potential exhibited by Oregano EO can be explained by its high carvacrol content. As it was explained above, the carvacrol displaces cholesterol molecules in the cell membrane [53]. Furthermore, the cholesterol has an important role in viral entry, membrane fusion, and lipid rafts, which are required for entry of the viral particle by endocytosis to its host cell, specifically for CHIKV [56]. It has been recently verified that carvacrol significantly reduced chIFITM3 gene expression that encodes the chicken interferon-inducible transmembrane protein, interleukin 6 (IL-6) and alpha-1 acid glycoprotein (α1-AGP) levels, leucocytic response, in other aspects, when pretreated broilers were experimentally infected by bronchitis virus (IBV) [15]. EOs act directly on the respiratory, circulatory, and central nervous systems through the skin and respiratory tract, and the administration in spray has recently been considered as a new strategy of EOs therapeutic application [59]. Recently, nasal IVM spray administration in a pig model has been showed to attaining high drug concentrations in nasopharyngeal tissue, a primary site of aerosol spread virus entrance/replication [43]. In this study we have demonstrated the synergy among components IVM, phthFGL and Oregano EO which act through different mechanisms of action against CHIKV, ZIKV and HHV-2 in vitro.

A comparison of pharmacokinetics parameters simulated with the webserver SWISSADME for phthFGL (**1a**, Fig. 1) and the commercial drug Ecabet sodium (**2**, Fig. 1) features similar and good druglikeness characteristics (see supplementary information, Figures S1 and S2). This supports phthFGL as a good lead candidate for the development of new broad-spectrum antivirals, which encourages further studies to improve the compound's physicochemical properties (solubility, pH=7.4 < 0.1 μg/mL). In fact, we checked the good pharmacokinetic profile of phthFGL through in vitro ADME studies (Tables S1 and S2, SI) following standard methods as reported previously by us and using various known drugs as controls [60].

5. Conclusions

Arboviruses and respiratory viruses can produce very similar clinical symptoms in the first days of the disease, hindering clinical diagnosis by health workers, creating problems for appropriate and early case management, and sometimes triggering fatal events. Studies of drug combinations with broad-spectrum antiviral activity, as described in this report, provide a step towards more effective drugs against diseases caused by emerging viruses. In the future, further studies of drug-drug interactions with commercially available medications will enable individuals to quickly take some medications at home for a few days to prevent severe illness before being attended to by the governmental healthcare system. Continued research in this area is crucial for improving our ability to respond to emerging virus threats [61].

Supplementary Materials: The following supporting information can be downloaded at the website of this paper posted on Preprints.org. Figure S1: Swissadme analysis for compound **1a**; Figure S2: Swissadme analysis for compound **2**; Table S1: In vitro pharmacokinetic parameters for compound **1a**: Caco2 permeability; Table S2: In vitro pharmacokinetic parameters for compound **1a**: stability in microsomes and plasma.

Author Contributions: Conceptualization, L.B.-G.; methodology, L.B.-G. and F.R.; software, O.J.J.-J.; validation, L.B.-G.; formal analysis, L.B.-G., F.R. and O.J.J.-J.; investigation, L.B.-G., O.J.J.-J., F.R., W.E.M.-H. and M.A.G.-C.; resources, L.B.-G. and M.A.G.-C.; writing—original draft preparation, L.B.-G.; writing—review and editing, L.B.-G., O.J.J.-J., W.E.M.-H., F.R. and M.A.G.-C.; supervision, L.B.-G. and M.A.G.-C.; project administration, L.B.-G., F.R. and M.A.G.-C.; funding acquisition, L.B.-G., F.R. and M.A.G.-C. All authors have read and agreed to the published version of the manuscript.

Funding: This research and the APC was funded by the regional government "Generalitat Valenciana, Conselleria de Educación, Universidades y Empleo", grant number CIAICO/2022/220. The Universitat Politecnica de Valencia also funded this research under a cooperation "ADSIDEO" research grant (AD1902). The

financial support was also provided by the Colombian government "Colciencias, Patrimonio Autónomo del Fondo Nacional de Financiamiento para la Ciencia, la Tecnología y la Innovación, Francisco José de Caldas-Colombia", grant 744 2016 (contract 648- 2017/project 111574455595) and "CODI, Comité para el Desarrollo de la Investigación-Universidad de Antioquia", grant "Apoyo a la Internacionalización de la Ciencia, Vicerrectoria de Investigacion UdeA" and the Board of Regents Support Fund Award LEQSF-RD-A-05.

Institutional Review Board Statement: Not applicable.

Informed Consent Statement: Not applicable.

Data Availability Statement: The data is available in the manuscript and the Supporting Information of this article. Raw data are available upon request.

Acknowledgments: The authors acknowledge the virology groups of "Universidad de Antioquia-Facultad de Medicina" and "Dirección de Redes en Salud Publica, Instituto Nacional de Salud, Bogotá, DC, Colombia" for providing the viruses. We extend our acknowledgements to the staff of the characterization department of the "Instituto de Tecnología Química (ITQ), UPV-CSIC" represented by Ms Estrella Mateos Otero, Ms Maria Isabel Tadeo Taboas and Ms Carmen Clemente Martínez and the administration department represented by Mr Antonio Corma Canos, Mr Guillermo Aparicio Adelantado, Ms Clara Fornés Mifsud and Ms Inmaculada Cubas Moreno; thanking also the management department for the necessary official burocracy represented by Ms Mónica Asunción Albelda, Mr Marcos Castillo Villena and Ms Inmaculada García Alfonso. Finally, we are grateful to any other member of the ITQ whose help was necessary for the development of this research.

Conflicts of Interest: L.B.-G. and M.A.G.-C. are inventors on a patent application for the use of 18-(phthalimid-2-yl)ferruginol as antiviral agent. González-Cardenete, M. A.; Betancur-Galvis, L. A. Spanish Patent ES 2586505, 2016; González-Cardenete, M. A.; Betancur-Galvis, L. A. PCT Patent WO 2016142568, 2016.

Sample Availability: Sample of compound **1a** is available from the authors.

References

1. Crump, A. Ivermectin: enigmatic multifaceted 'wonder' drug continues to surprise and exceed expectations. *J. Antibiot.* **2017**, *70*, 495–505. https://doi.org/10.1038/ja.2017.11
2. Caly, L.; Druce, J.D.; Catton, M.G.; Jans, D.A.; Wagstaff, K.M. The FDA-approved drug ivermectin inhibits the replication of SARS-CoV-2 in vitro. *Antiviral Res.* **2020**, *178*, 104787. https://doi.org/10.1016/j.antiviral.2020.104787
3. Heidary, F.; Gharebaghi, R. Ivermectin: a systematic review from antiviral effects to COVID-19 complementary regimen. *J. Antibiot.* **2020**, *73*, 593–602. https://doi.org/10.1038/s41429-020-0336-z
4. Wagstaff, K.M.; Sivakumaran, H.; Heaton, S.M.; Harrich, D.; Jans, D.A. Ivermectin is a specific inhibitor of importin α/β-mediated nuclear import able to inhibit replication of HIV-1 and dengue virus, *Biochem. J.* **2012**, *443*, 851–856. https://doi.org/10.1042/bj20120150
5. Yang, S.N.Y.; Atkinson, S.C.; Wang, C.; Lee, A.; Bogoyevitch, M.A.; Borg, N.A.; Jans, D.A. The broad spectrum antiviral ivermectin targets the host nuclear transport importin α/β1 heterodimer. *Antiviral Res.* **2020**, *177*, 104760. https://doi.org/10.1016/j.antiviral.2020.104760
6. Martin A.J.; Jans, D.A. Antivirals that target the host IMPα/β1-virus interface. *Biochem. Soc. Tran.* **2021**, 49, 281–295. https://doi.org/10.1042/bst20200568
7. Chandrakala, V.; Aruna, V.; Angajala, G.; Reddy, P.G. Chemical Composition and Pharmacological Activities of Essential Oils. In Essential oils: extraction methods and applications; Inamuddin, Ed.; Scrivener publishing LLC: Bervely, USA, 2023; chapter 11, pp. 229-268. https://doi.org/10.1002/9781119829614.ch11
8. Schnitzler, P. Essential oils for the treatment of herpes simplex virus infections. *Chemotherapy* **2019**, *64*, 1–7. https://doi.org/10.1159/000501062
9. Lai, W.-L.; Chuang, H.-S.; Lee, M.-H.; Wei, C.-L.; Lin, C.-F.; Tsai, Y.-C. Inhibition of herpes simplex virus type 1 by thymol-related monoterpenoids. *Planta Med.* **2012**, *78*, 1636–1638. https://doi.org/10.1055/s-0032-1315208
10. Brand, Y.M.; Roa-Linares, V.C.; Betancur-Galvis, L.A.; Durán-García, D.C.; Stashenko, E. Antiviral activity of colombian Labiatae and Verbenaceae family essential oils and monoterpenes on human herpes viruses. *J. Essent. Oil Res.* **2016**, *28*, 130–137. https://doi.org/10.1080/10412905.2015.1093556
11. Mustafa, A.; El-Kashef, D.H.; Abdelwahab, M.F.; Gomaa, A.A.-R.; Mustafa, M.; Abdel-Wahab, N.M.; Ibrahim, A.H. Investigation of antiviral effects of essential oils. In Essential oils: extraction methods and

applications; Inamuddin, Ed.; Scrivener publishing LLC: Bervely, USA, 2023; chapter 5, pp. 99-124. https://doi.org/10.1002/9781119829614.ch5

12. Da Silva, J.K.R.; Figueiredo, P.L.B.; Byler, K.G.; Setzer, W.N. Essential oils as antiviral agents, potential of essential oils to treat SARS-CoV-2 infection: an in-silico investigation. *Int. J. Mol. Sci.* **2020**, *21*, 3426. https://doi.org/10.3390/ijms21103426
13. Wani, A.R.; Yadav, K.; Khursheed, A.; Rather, M.A. An updated and comprehensive review of the antiviral potential of essential oils and their chemical constituents with special focus on their mechanism of action against various influenza and coronaviruses. *Microb. Pathog.* **2021**, *152*, 104620. https://doi.org/10.1016/j.micpath.2020.104620
14. Serifi, I.; Tzima, E.; Bardouki, H.; Lampri, E.; Papamarcaki, T. Effects of the essential oil from *Pistacia lentiscus* var. *chia* on the lateral line system and the gene expression profile of zebrafish (*Danio rerio*). *Molecules* **2019**, *24*, 3919. https://doi.org/10.3390/molecules24213919
15. Sawerus, M.G.; Shehata, O.; Ahmed, W.M.S.; Shany, S.; Hassan, K.E.; Mahdi, E.A.; Mohamed, A.H. The modulatory effect of carvacrol on viral shedding titer and acute phase response in broiler chickens experimentally infected with infectious bronchitis virus. *Microb. Pathog.* **2022**, *163*, 105410. https://doi.org/10.1016/j.micpath.2022.105410
16. González, M. A. Aromatic abietane diterpenoids: their biological activity and synthesis. *Nat. Prod. Rep.* **2015**, *32*, 684–704. http://dx.doi.org/10.1039/c4np00110a
17. Chan, E.W.C.; Wong, S.K.; Chan, H.T. Ferruginol and sugiol: a short review of their chemistry, sources, contents, pharmacological properties and patents. *Trop. J. Nat. Prod. Res.* **2023**, *7*, 2325-2336, http://www.doi.org/10.26538/tjnpr/v7i2.4
18. Roa-Linares, V.C.; Brand, Y.M.; Agudelo-Gomez, L.S.; Tangarife-Castaño, V.; Betancur-Galvis, L.A.; Gallego-Gomez, J.C.; González, M.A. Anti-herpetic and anti-dengue activity of abietane ferruginol analogues synthesized from (+)-dehydroabietylamine. *Eur. J. Med. Chem.* **2016**, *108*, 79–88. https://doi.org/10.1016/j.ejmech.2015.11.009
19. Sousa, F.T.G.; Nunes, C.; Romano, C. M.; Sabino, E. C.; González-Cardenete, M. A. Anti-Zika virus activity of several abietane-type ferruginol analogues. *Rev. Inst. Med. Trop. São Paulo* **2020**, *62*, e97. https://dx.doi.org/10.1590/S1678-9946202062097
20. González-Cardenete, M.A.; Hamulić, D.; Miquel-leal, F.J.; González-Zapata, N.; Jimenez-Jarava, O.J.; Brand, Y.M.; Restrepo-Mendez, L.C.; Martinez-Gutierrez, M.; Betancur-Galvis, L.A.; Marín, M.L. Antiviral profiling of C18- or C19-functionalized semisynthetic abietane diterpenoids. *J. Nat. Prod.* **2022**, *85*, 2044–2051. https://doi.org/10.1021/acs.jnatprod.2c00464
21. Varbanov, M.; Philippot, S.; González-Cardenete, M.A. Anticoronavirus evaluation of antimicrobial diterpenoids: application of new ferruginol analogues. *Viruses* **2023**, *15*, 1342. https://doi.org/10.3390/v15061342
22. Roa-Linares, V.C.; Escudero-Flórez M.; Vicente-Manzanares, M.; Gallego-Gómez J.C. Host cell targets for unconventional antivirals against RNA viruses. *Viruses* **2023**, 15, 776. https://doi.org/10.3390/v15061342
23. González, M. A. Synthetic derivatives of aromatic abietane diterpenoids and their biological activities. *Eur. J. Med. Chem.* **2014**, *87*, 834–842. http://dx.doi.org/10.1016/j.ejmech.2014.10.023
24. Yarovaya, O.I.; Laev, S.S.; Salakhutdinov, N.F. Antiviral properties of diterpenes and their derivatives. *Russ. Chem. Rev.* **2023**, *92*, RCR5056. https://doi.org/10.57634/RCR5056
25. Lakshmanan, M. Drugs used in acid peptic disorders. In Introduction to Basics of Pharmacology and Toxicology: Essentials of Systemic Pharmacology: From Principles to Practice; Paul, A.; Anandabaskar, N.; Mathaiyan, J.; Raj, G.M., Eds.; Springer: Singapore, 2021; vol. 2, pp. 553–567. https://doi.org/10.1007/978-981-33-6009-9_34
26. Shyr, Z.A.; Cheng, Y.-S.; Lo, D.C.; Zheng, W. Drug combination therapy for emerging viral diseases. *Drug Discov. Today* **2021**, *26*, 2367–2376. https://doi.org/10.1016/j.drudis.2021.05.008
27. Wagoner, J.; Herring, S.; Hsiang, T.-Y.; Ianevski, A.; Biering, S.B.; Xu, S.; Hoffmann, M.; Pöhlmann, S.; Gale Jr., M.; Aittokallio, T.; Schiffer, J.T.; White, J.M.; Polyak, S.J. Combinations of host- and virus-targeting antiviral drugs confer synergistic suppression of SARS-CoV-2. *Microbiol. Spectr.* **2022** , *10*, e0333122. https://doi.org/10.1128/spectrum.03331-22
28. Pan American Health Organization. Recommendations for Laboratory Detection and Diagnosis of Arbovirus Infections in the Region of the Americas; Pan American Health Organization: Washington, D.C., 2023. Available online: https://iris.paho.org/handle/10665.2/57555

29. Schalkwijk, H.H.; Snoeck, R.; Andrei, G. Acyclovir resistance in herpes simplex viruses: prevalence and therapeutic alternatives. *Biochem Pharmacol.* **2022**, 206, 115322. https://doi.org/10.1016/j.bcp.2022.115322
30. Sadowski, L.A.; Upadhyay, R.; Greeley, Z.W.; Margulies, B.J. Current drugs to treat infections with herpes simplex viruses-1 and -2. *Viruses* **2021**, *13*, 1228. https://doi.org/10.3390/v13071228
31. Laiton-Donato, K.; Álvarez-Díaz, D.A.; Rengifo, A.C.; Torres-Fernández, O.; Usme-Ciro, J.A.; Rivera, J.A.; Santamaría, G.; Naizaque, J.; Monroy-Gómez, J.; Sarmiento, L.; Gunturiz, M.L.; Muñoz, A.; Vanegas, R.; Rico, A.; Pardo, L.; Peláez-Carvajal D. Complete genome sequence of Colombian Zika virus strain obtained from BALB/c mouse brain after intraperitoneal inoculation. *Microbiol. Resour. Announc.* **2019**, *8*, e01719–18. https://dx.doi.org/10.1128/MRA.01719-18
32. Vlietinck, A.J.; Van Hoof, L.; Totté, J.; Lasure, A.; Vanden Berghe, D.; Rwangabo, P.C.; Mvukiyumwami, J. Screening of hundred Rwandese medicinal plants for antimicrobial and antiviral properties. *J. Ethnopharmacology* **1995**, *46*, 31–47. https://doi.org/10.1016/0378-8741(95)01226-4
33. Daina, A.; Michielin, O.; Zoete, V. SwissADME: a free web tool to evaluate pharmacokinetics, drug-likeness and medicinal chemistry friendliness of small molecules. *Sci. Rep.* **2017**, *7*, 42717. https://doi.org/10.1038/srep42717
34. Pancheva, S.N. Potentiating effect of ribavirin on the anti-herpes activity of acyclovir. *Antiviral Res.* **1991**, 16, 151–161. https://doi.org/10.1016/0166-3542(91)90021-i
35. Shishkov, S.; Pancheva S. The synergistic antiviral effect of acyclovir and ribavirin against the herpes simplex type-1 virus and the pseudorabies virus in vitro. *Acta Microbiol. Bulg.* **1990**, *25*, 69–75.
36. Azam, F.; Taban, I.M.; Eid, E.E.M.; Iqbal, M.; Alam, O.; Khan, S.; Mahmood, D.; Anwar, M.J.; Khalilullah, H.; Khan, M.U. An *in-silico* analysis of ivermectin interaction with potential SARS-CoV-2 targets and host nuclear importin α. *J. Biomol. Struct. Dyn.* **2022**, 40, 2851–2864. https://doi.org/10.1080/07391102.2020.1841028
37. Jermain, B.; Hanafin, P.O.; Cao, Y.; Lifschitz, A.; Lanusse, C.; Rao, G.G. Development of a minimal physiologically-based pharmacokinetic model to simulate lung exposure in humans following oral administration of ivermectin for COVID-19 drug repurposing. *J. Pharm. Sci.* **2020**, *109*, 3574–3578. https://doi.org/10.1016/j.xphs.2020.08.024
38. Ahmed, S.; Karim, M.M.; Ross, A.G.; Hossain, M.S.; Clemens, J.D.; Sumiya, M.K.; Phru, C.S.; Rahman, M.; Zaman, K.; Somani, J.; Yasmin R, Hasnat, M.A.; Kabir, A.; Aziz, A.B.; Khan, W.A. A five-day course of ivermectin for the treatment of COVID-19 may reduce the duration of illness. *Int. J. Infect. Dis.* **2021**, *103*, 214–216. https://doi.org/10.1016/j.ijid.2020.11.191
39. Suputtamongkol, Y.; Avirutnan, P.; Mairiang, D.; Angkasekwinai, N.; Niwattayakul, K.; Yamasmith, E.; Saleh-Arong, F.A.; Songjaeng, A.; Prommool, T.; Tangthawornchaikul, N.; Puttikhunt, C.; Hunnangkul, S.; Komoltri, C.; Thammapalo, S.; Malasit P. Ivermectin accelerates circulating nonstructural protein 1 (NS1) clearance in adult dengue patients: a combined phase 2/3 randomized double-blinded placebo controlled trial. *Clin. Infect. Dis*. **2021**, *72*, e586–e593. https://doi.org/10.1093/cid/ciaa1332
40. Tay, M.Y.; Fraser, J.E.; Chan, W.K.; Moreland, N.J.; Rathore, A.P.; Wang, C.; Vasudevan, S.G.; Jans, D.A. Nuclear localization of dengue virus (DENV) 1-4 non-structural protein 5; protection against all 4 DENV serotypes by the inhibitor Ivermectin. *Antiviral Res.* **2013**, *99*, 301–306. https://doi.org/10.1016/j.antiviral.2013.06.002
41. Jitobaom, K.; Boonarkart, C.; Manopwisedjaroen, S.; Punyadee, N.; Borwornpinyo, S.; Thitithanyanont, A.; Avirutnan, P.; Auewarakul P. Synergistic anti-SARS-CoV-2 activity of repurposed anti-parasitic drug combinations. *BMC Pharmacol. Toxicol.* **2022**, *23*, 41. https://doi.org/10.1186/s40360-022-00580-8
42. Tan, Y.L.; Tan, K.S.W.; Chu, J.J.H.; Chow, V.T. Combination treatment with remdesivir and ivermectin exerts highly synergistic and potent antiviral activity against murine coronavirus infection. *Front. Cell Infect. Microbiol*. **2021**, *11*, 700502. https://doi.org/10.3389/fcimb.2021.700502
43. Errecalde, J.; Lifschitz, A.; Vecchioli, G.; Ceballos, L.; Errecalde, F.; Ballent, M.; Marín, G.; Daniele, M.; Turic, E.; Spitzer, E.; Toneguzzo, F.; Gold, S.; Krolewiecki, A.; Alvarez, L.; Lanusse, C. Safety and pharmacokinetic assessments of a novel ivermectin nasal spray formulation in a pig model. *J. Pharm. Sci.* **2021**, *110*, 2501–2507. https://doi.org/10.1016/j.xphs.2021.01.017
44. Varghese, F.S.; Kaukinen, P.; Gläsker, S.; Bespalov, M.; Hanski, L.; Wennerberg, K.; Kümmerer, B.M.; Ahola, T. Discovery of berberine, abamectin and ivermectin as antivirals against chikungunya and other alphaviruses. *Antivir. Res.* **2016**, *126*, 117–124. https://doi.org/10.1016/j.antiviral.2015.12.012

45. Słońska, A.; Cymerys, J.; Skwarska, J.; Golke, A.; Bańbura, M.W. Influence of importin alpha/beta and exportin 1 on equine herpesvirus type 1 (EHV-1) replication in primary murine neurons. *Pol. J. Vet. Sci.* **2013**, *16*, 749–751. https://doi.org/10.2478/pjvs-2013-0106
46. Lv, C.; Liu, W.; Wang, B.; Dang, R.; Qiu, L.; Ren, J.; Yan, C.; Yang, Z.; Wang, X. Ivermectin inhibits DNA polymerase UL42 of pseudorabies virus entrance into the nucleus and proliferation of the virus in vitro and vivo. *Antiviral Res.* **2018**, *159*, 55–62. https://doi.org/10.1016/j.antiviral.2018.09.010
47. Döhner, K.; Ramos-Nascimento, A.; Bialy, D.; Anderson, F.; Hickford-Martinez, A.; Rother, F.; Koithan, T.; Rudolph, K.; Buch, A.; Prank, U.; Binz, A.; Hügel, S.; Lebbink, R.J.; Hoeben, R.C.; Hartmann, E.; Bader, M.; Bauerfeind, R.; Sodeik, B. Importin α1 is required for nuclear import of herpes simplex virus proteins and capsid assembly in fibroblasts and neurons. *PLoS Pathog.* **2018**, *14*, e1006823. https://doi.org/10.1371/journal.ppat.1006823
48. Kim, J.Y.; Kim, D.H.; Min, K.A.; Maeng, H.-J.; Jang, D.-J.; Cho, K.H. Preparation, characterization, and i*n vitro* release of chitosan-ecabet electrolyte complex for the mucosal delivery. *J. Nanosci. Nanotechnol.* **2019**, *19*, 640–645. https://doi.org/10.1166/jnn.2019.15961
49. Zhang, D.; Du, X.; Liu, M.; Li, H.; Jiang, Y.; Zhao, L.; Gu, J. Determination of ecabet in human plasma by high-performance liquid chromatography-tandem mass spectrometry. *J. Chromatogr. B Analyt Technol. Biomed. Life Sci.* **2008**, *863*, 223–228. https://doi.org/10.1016/j.jchromb.2008.01.013
50. Wei, Y.; He, J.; Qin, H.; Wu, X.; Yao, X. Determination of ferruginol in rat plasma via high-performance liquid chromatography and its application in pharmacokinetics study. *Biomed. Chromatogr.* **2009**, *23*, 1116–1120. https://doi.org/10.1002/bmc.1232
51. De Forni, D.; Poddesu, B.; Cugia, G.; Chafouleas, J.; Lisziewicz, J.; Lori, F. Synergistic drug combinations designed to fully suppress SARS-CoV-2 in the lung of COVID-19 patients. *PLoS One* **2022**, *17*, e0276751. https://doi.org/10.1371/journal.pone.0276751
52. Vanpouille, C.; Lisco, A.; Introini, A.; Grivel, J.C.; Munawwar, A.; Merbah, M.; Schinazi, R.F.; Derudas, M.; McGuigan, C.; Balzarini, J.; Margolis, L. Exploiting the anti-HIV-1 activity of acyclovir: suppression of primary and drug-resistant HIV isolates and potentiation of the activity by ribavirin. *Antimicrob. Agents Chemother.* **2012**, *56*, 2604–2611. https://doi.org/10.1128/aac.05986-11
53. Mediouni, S.; Jablonski, J.A.; Tsuda, S.; Barsamian, A.; Kessing, C.; Richard, A.; Biswas, A.; Toledo, F.; Andrade, V.M.; Even, Y.; Stevenson, M.; Tellinghuisen, T.; Choe, H.; Cameron, M.; Bannister, T. D.; Valente, S. T. Oregano oil and its principal component, carvacrol, inhibit HIV-1 fusion into target cells. *J. Virol.* **2020**, *94*, e00147-20. https://doi.org/10.1128/JVI.00147-20
54. Lai, W.-L.; Chuang, H.-S.; Lee, M.-H.; Wei, C.-L.; Lin, C.-F.; Tsai, Y.-C. Inhibition of herpes simplex virus type 1 by thymol-related monoterpenoids. *Planta Med.* **2012**, *78*, 1636–1638. https://doi.org/10.1055/s-0032-1315208
55. Shah, M.; Kumar, S. Role of cholesterol in anatid herpesvirus 1 infections in vitro. *Virus Res.* **2020**, *290*, 198174. https://doi.org/10.1016/j.virusres.2020.198174
56. Glitscher, M.; Hildt, E. Endosomal Cholesterol in Viral Infections - A Common Denominator? *Front Physiol.* **2021**, *12*, 750544. https://doi.org/10.3389/fphys.2021.750544
57. Martínez-Gutierrez M.; Castellanos, J.E.; Gallego-Gómez, J.C. Statins reduce dengue virus production via decreased virion assembly. *Intervirology* **2011**, *54*, 202–216. https://doi.org/10.1159/000321892
58. Betancur-Galvis, L.A.; Jimenez-Jarava, O.J. Actividad anti-chikungunya de los aceites esenciales de plantas pertenecientes a las familias verbenaceae, piperaceae, poaceae, lamiaceae, lauraceae y myrtaceae: estudios de docking molecular. In Entre Ciencia e Ingenieria 4; Pereira da Silva, A.F. Ed.; Atena Editora: Ponta Grossa, Brazil, 2022; Chapter 1, pp 1–24. https://doi.org/10.22533/at.ed.863221910
59. Zhong, Y.; Zheng, Q.; Hu, P.; Huang, X.; Yang, M.; Ren, G.; Du, Q.; Luo, J.; Zhang, K.; Li, J.; Wu, H.; Guo, Y.; Liu, S. Sedative and hypnotic effects of compound Anshen essential oil inhalation for insomnia. *BMC Complement. Altern. Med.* **2019**, *19*, 306. https://doi.org/10.1186/s12906-019-2732-0
60. Ling, T.; Tran, M.; González, M.A.; Gautam, L.N.; Connelly, M.; Wood, R.K.; Fatima, I.; Miranda-Carboni, G.; Rivas, F. (+)-Dehydroabietylamine derivatives target triple-negative breast cancer. *Eur. J. Med. Chem.* **2015**, *102*, 9–13. https://doi.org/10.1016/j.ejmech.2015.07.034
61. Brogi, S. Novel antiviral agents: synthesis, molecular modelling studies and biological investigation. *Viruses* **2023**, *15*, 2042. https://doi.org/10.3390/v15102042

 doi:10.20944/preprints202310.0781.v1

disclaim responsibility for any injury to people or property resulting from any ideas, methods, instructions or products referred to in the content.